
AFRL-ML-TY-TP-2002-4515

# GROUND PENETRATING RADAR SIGNAL PROCESSING TECHNIQUES FOR AIRFIELD EVALUATIONS (POSTPRINT)

Jeffrey H. Meloy, Charles H. Overman, and James L. Kurtz
University of Florida
Electronic Communications Laboratory
PO Box 140245
Gainesville, FL 32614-0245

Jonathan R. Porter
Air Force Research Laboratory
Materials and Manufacturing Directorate
Airbase Technologies Division
139 Barnes Dr., Ste 2
Tyndall AFB, FL 32403-5323

James H. Greene
Applied Research Associates, Inc.
421 Oak Drive
Panama City, FL 32401

July 2002



**AIR FORCE RESEARCH LABORATORY**
**MATERIALS AND MANUFACTURING DIRECTORATE**

■ **Air Force Materiel Command** ■ **United States Air Force** ■ **Tyndall Air Force Base, FL 32403-5323**

# REPORT DOCUMENTATION PAGE

*Form Approved*
*OMB No. 0704-0188*



**PLEASE DO NOT RETURN YOUR FORM TO THE ABOVE ADDRESS.**

| 1. REPORT DATE *(DD-MM-YYYY)* | 2. REPORT TYPE | 3. DATES COVERED *(From - To)* |
|---|---|---|
| 30-JUL-2002 | Journal Article - POSTPRINT | |

**4. TITLE AND SUBTITLE**

Ground Penetrating Radar Signal Processing Techniques for Airfield Evaluations (POSTPRINT)

**5a. CONTRACT NUMBER**

**5b. GRANT NUMBER**

**5c. PROGRAM ELEMENT NUMBER**

**6. AUTHOR(S)**

Jeffrey H. Meloy*, Charles H. Overman*, James L. Kurtz*, Jonathan R. Porter^, James H. Greene%
Applied Research Associates, Inc.
421 Oak Drive
Panama City, FL 32401

**5d. PROJECT NUMBER**

**5e. TASK NUMBER**

**5f. WORK UNIT NUMBER**

**7. PERFORMING ORGANIZATION NAME(S) AND ADDRESS(ES)**

*University of Florida; Electronic Communications Laboratory; PO Box 140245; Gainesville, Florida 32614-0245
%Applied Research Associates, Inc. ; 421 Oak Drive; Panama City, FL 32401

**8. PERFORMING ORGANIZATION REPORT NUMBER**

**9. SPONSORING/MONITORING AGENCY NAME(S) AND ADDRESS(ES)**

^Air Force Research Laboratory
Materials and Manufacturing Directorate
Airbase Technologies Division
139 Barnes Drive, Suite 2
Tyndall Air Force Base, FL 32403-5323

**10. SPONSOR/MONITOR'S ACRONYM(S)**

AFRL/MLQ

**11. SPONSOR/MONITOR'S REPORT NUMBER(S)**

AFRL-ML-TY-TP-2002-4515

**12. DISTRIBUTION/AVAILABILITY STATEMENT**

DISTRIBUTION A. Approved for public release; distribution unlimited.
Available only to DTIC users. U.S. Government or Federal Purpose Rights License.

**13. SUPPLEMENTARY NOTES**

Distribution Code 20: JOURNAL ARTICLES; DTIC USERS ONLY. This paper was published in SPIE Proceedings Vol. 4744. Radar Sensor Technology and Data Visualization, Nickolas L. Faust; James L. Kurtz; Robert Trebits, Editors, pp.37-47

**14. ABSTRACT**

The University of Florida, Electronic Communications Laboratory (ECL), as part of a project with the Air Force Research Laboratory (AFRL), is investigating the utility of ground penetrating radar (GPR) for airfield evaluations. It is expected that the GPR and the results of current research will assist the Air Force in assessing airfields with less coring and allow more rapid and accurate airfield evaluations by providing continuous estimates of the pavement and subsurface conditions. AFRL has conducted airfield measurements using a high-resolution GPR mounted on a test van. Using time domain data from a pair of ground-coupled antennas, one in bistatic mode and the other in monostatic mode, the thickness of pavement and other subsurface layers can be estimated. In order for GPR to be useful for airfield evaluations, practical considerations such as automated data processing capability and efficient data analysis procedures have also been addressed. This paper will describe novel approaches and signal processing techniques developed for detecting layer interface boundaries and estimating the layer properties using GPR. In addition, the software tools developed to facilitate airfield evaluations will be discussed. Finally, surface layer thickness estimates will be compared to measured cores from a recent airfield assessment.

**15. SUBJECT TERMS**

ground penetrating radar, radar signal processing, radar detection

| 16. SECURITY CLASSIFICATION OF: | | | 17. LIMITATION OF ABSTRACT | 18. NUMBER OF PAGES | 19a. NAME OF RESPONSIBLE PERSON |
|---|---|---|---|---|---|
| a. REPORT | b. ABSTRACT | c. THIS PAGE | | | Jonathan R. Porter |
| U | U | U | UU | 11 | 19b. TELEPHONE NUMBER *(Include area code)* 850 283 6002 |

Reset

**Standard Form 298** (Rev. 8/98)
Prescribed by ANSI Std. Z39.18

# Ground penetrating radar signal processing techniques for airfield evaluations

Jeffrey H. Meloy*[a], Charles H. Overman IV[a], James L. Kurtz[a]
Jonathan R. Porter**[b], James H. Greene***[c]
[a]University of Florida, Electronic Communications Laboratory;
[b]U.S. Air Force Research Laboratory; [c]Applied Research Associates

## ABSTRACT

The University of Florida, Electronic Communications Laboratory (ECL), as part of a project with the Air Force Research Laboratory (AFRL), is investigating the utility of ground penetrating radar (GPR) for airfield evaluations. It is expected that the GPR and the results of current research will assist the Air Force in assessing airfields with less coring and allow more rapid and accurate airfield evaluations by providing continuous estimates of the pavement and subsurface conditions. AFRL has conducted airfield measurements using a high-resolution GPR mounted on a test van. Using time domain data from a pair of ground-coupled antennas, one in bistatic mode and the other in monostatic mode, the thickness of pavement and other subsurface layers can be estimated. In order for GPR to be useful for airfield evaluations, practical considerations such as automated data processing capability and efficient data analysis procedures have also been addressed. This paper will describe novel approaches and signal processing techniques developed for detecting layer interface boundaries and estimating the layer properties using GPR. In addition, the software tools developed to facilitate airfield evaluations will be discussed. Finally, surface layer thickness estimates will be compared to measured cores from a recent airfield assessment.

**Keywords:** ground penetrating radar, radar signal processing, radar detection

## 1. BACKGROUND

Currently, the Air Force Civil Engineering Support Agency (AFCESA) and other Air Force personnel perform airfield studies ranging from basic field investigations to detailed and complex airfield pavement evaluations required by the U.S. Air Force Airfield Evaluation Program[1]. The purpose of this program is to determine the condition of all airfields used by present or potential Air Force missions. Current pavement and subsurface field assessment methods include core drilling, visual observations, and obtaining measurements using a heavy weight deflectometer (HWD) and a soil penetration device such as a dynamic cone penetrometer (DCP). These methods are time consuming and can fail to provide the sampling resolution needed to correctly characterize the surrounding pavement and subsurface conditions, track changes in the pavement and subsurface, or identify localized problem areas underneath the pavement. GPR has the potential to improve airfield evaluations by allowing more continuous and rapid data collections than the current evaluation methods. When combined with current evaluation techniques GPR will enable better decisions and help provide a more accurate and complete analysis of the pavement subsurface.

GPR is a short-range sensor that is used to measure the electromagnetic reflections from an ultra-wideband radar impulse. The observed amplitude changes in the received time response waveform are due to the abrupt changes in the electrical properties of a layered medium or reflections from buried objects[2]. Antennas used for GPR typically have a beamwidth of 90 degrees or more. This can make the position of an object or layer very difficult to determine when considering only a single radar return. Therefore, GPR data is typically collected along a straight path in evenly spaced intervals using a distance measuring instrument (usually a survey wheel) as a trigger.

*jmeloy@ecl.ufl.edu; phone 1 352 392-9645; University of Florida, Electronic Communications Laboratory, PO Box 140245, Gainesville, Florida 32614-0245; **Jon.Porter@tyndall.af.mil.; ***Jamie.Greene@tyndall.af.mil

Radar Sensor Technology and Data Visualization, Nickolas L. Faust, James L. Kurtz,
Robert Trebits, Editors, Proceedings of SPIE Vol. 4744 (2002) © 2002 SPIE · 0277-786X/02/$15.00

The ECL has worked with the Florida Department of Transportation (FDOT) for several years to improve the usability and accuracy of GPR for roadway analysis[3,4]. The potential utility of GPR for pavement measurements has been only partially realized for airfield applications. Several obstacles have prevented wider GPR utilization, including the large amounts of data that need to be collected by the GPR to map an entire airfield, the significant amount of operator interaction and interpretation required, and the vast amount of signal processing that is required. These obstacles have tended to make GPR under-utilized, even in those cases where adequate measurement accuracies have been possible. The goal of the current research is to improve the usability and accuracy of GPR for airfield assessments.

## 2. GPR ANALYSIS SOFTWARE

As part of the previous work for the FDOT, a comprehensive GPR analysis software tool was developed at the ECL. The GPR software was designed and constructed to improve GPR evaluation by providing better interaction with the data and by increasing layer property estimation accuracy to reduce subjective operator analysis. The software is driven by a Graphical User Interface (GUI) and provides a multitude of functions for GPR data processing, visualization, and data management. For airfield assessments, modifications were made to the GPR analysis software to accommodate the AFRL's current and potential GPR hardware. Also, software tools were added for batch processing and summary analysis report creation for entire airfields. Finally, import and display capabilities were implemented for core log files and data from HWD and DCP sensors. Figure 1 below shows the main interface of the GPR analysis software.

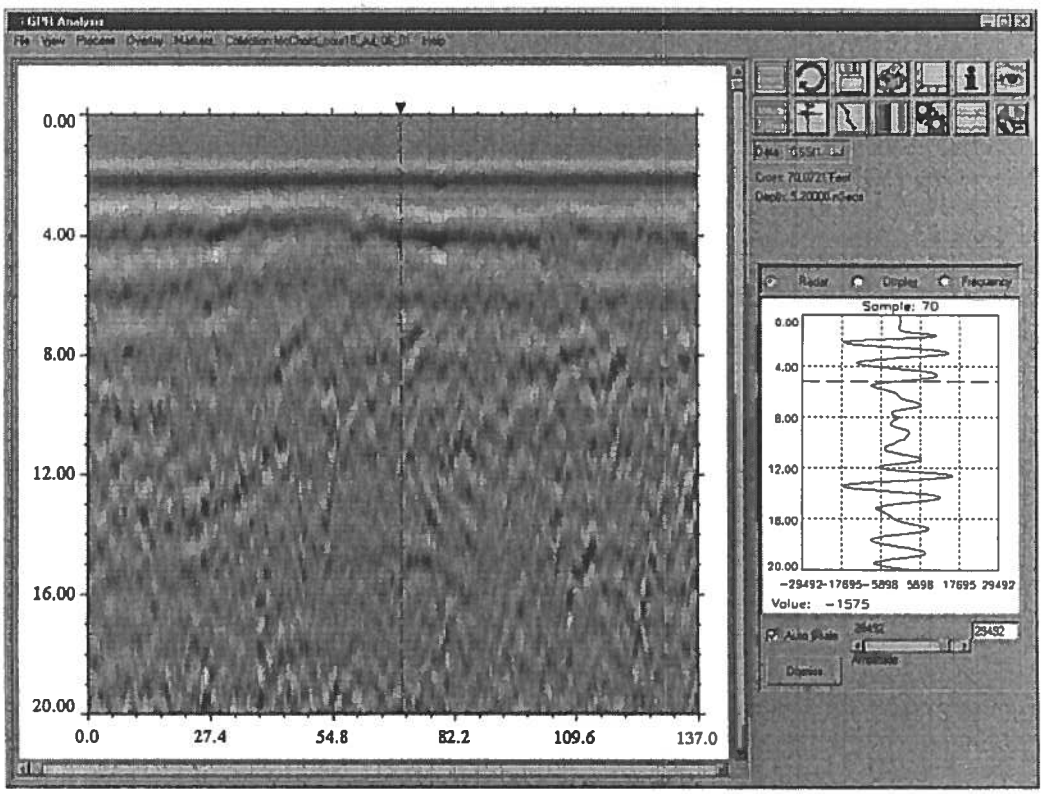


Figure 1. GPR analysis software

## 3. GPR SIGNAL PROCESSING OVERVIEW

The main processing objective for GPR data is to determine the properties of subsurface layers (asphalt, concrete, and the subgrade). Autonomous determination of these semi-continuous subsurface interfaces is a difficult task that greatly impacts GPR analysis efficiency. Manual selection of interface returns is labor intensive, emphasizing the need for algorithms that allow the bulk of this work to be handled by a computer. GPR signal processing attempts to remove much of the intensive human interaction and experience that is required. This will reduce the subjectivity of operator analysis and minimize processing cost by lowering the required operator training and experience. Several processing aspects are used to simplify GPR analysis. First, automated processing of GPR data will attempt to detect and segment layer interfaces. Next, properties of the layers will be computed, including layer thickness, relative dielectric permittivity ($\varepsilon_r$), and waveform propagation velocity. Finally, processing results can be displayed and summarized using the GPR analysis software.

Techniques for layer property determination are subject to the physics of the GPR phenomena. Layer thickness, for example, is estimated by measuring the delay and waveform velocity to each layer. Velocity is, therefore, a critical property which may be determined in different ways. Air-launched GPR systems can use the ratio of the return amplitudes from successive layers to estimate the reflection coefficient ($\rho$), $\varepsilon_r$ and velocity[3,5]. This calculation may, at times, be subject to recursive errors that originate with surface amplitude errors caused by surface roughness[4,6]. An alternative approach has been developed that uses the time-delay differences between two ground-coupled antennas. This method has the potential for improved velocity and $\varepsilon_r$ measurements, which will result in more accurate thickness calculations. However, processing data from the dual propagation path system presents its own unique challenges.

GPR data processing is done using a set of sequentially applied algorithms which automate the computation of the subsurface properties needed. Many of the algorithms operate as general purpose functional processing blocks that work independent of radar type or configuration. Other processing steps require algorithms that are tailored for specific systems or configurations. The processing flow, as indicated in Figure 2, has been designed and implemented in a modular fashion to facilitate algorithm development and performance comparisons using the GPR analysis software. Major processing steps include detecting radar returns, prescreening detects from layers, segmenting detects into interfaces, improving interface continuity, and calculation of layer parameters.

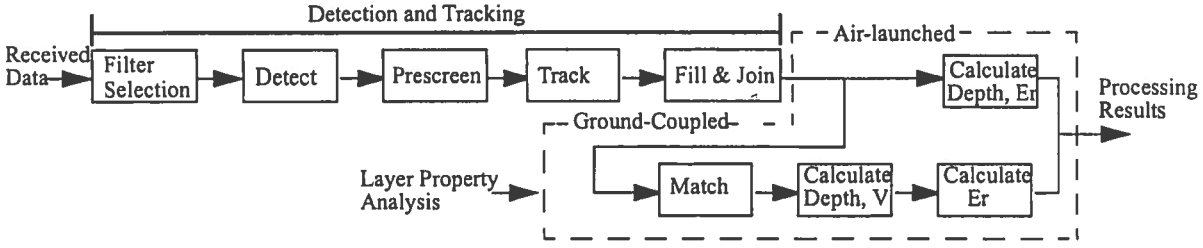


Figure 2. GPR signal processing flow diagram

## 4. DETECTION AND TRACKING

### 4.1 Filter selection

Matched filtering is a standard approach to conventional radar signal processing and is mathematically identical to a correlation receiver[7]. The matched-filter waveform is convolved with the received GPR waveform to maximize the signal-to-noise ratio (SNR). Determination of the appropriate matched filter to use for detection may be accomplished in different ways depending on the system configuration. The simplest way of acquiring a matched filter is to measure the transmitted pulse. The measured response from an isolated interface is time-inversed to create a matched-filter waveform. Measurement of an isolated interface response can be easily accomplished with an air-launched system. A metal plate may be placed on the pavement surface under the elevated air-launched antenna. The metal plate reflects all transmitted

energy and provides a measured return that is free from interference. Ground-coupled systems make field measurements of the transmitted waveform impractical due to the inability to easily isolate an interface return from the coupling response and interfering returns within the ground. To overcome this difficulty, a GPR testbed was constructed that allows the response from a metal plate through a homogenous media to be collected. Isolated interface responses were obtained using ten inches of concrete for each of AFRL's ground-coupled antennas. When processing a particular data set, the appropriate matched-filter waveform is selected based on the antenna identification listed in the GPR data header.

### 4.2 Detection

The received GPR signal resulting from a transmitted pulse, x(t), emerging from N-layers of isotropic and homogeneous media, such as surface and subsurface layers, can be written as

$$x_r(t) = \Sigma_{i=0}^{N} A_i x(t - t_i) + c(t) + n(t) \quad (1)$$

where $A_i$ represents the amplitude of the reflected pulse from layer $i$ at time $t_i$, $c(t)$ represents a noise component due to clutter responses, and $n(t)$ is a random noise process. Detection can be viewed as the process of finding the $A_i$ and $t_i$ from $x_r(t)$ in (1). Subsurface layers are defined as extended regions within the ground where abrupt changes in $\varepsilon_r$ occur. The change in $\varepsilon_r$ results in a large impulse response at the interface boundary. Layer interface detection attempts to obtain the location and amplitude of the ground response components associated with these subsurface layers. When GPR data is processed, the number of desired interfaces to detect is passed as a parameter to the algorithm.

An iterative matched-filter technique has been used to find the peak locations corresponding to interfaces by convolution of an antenna-specific matched-filter waveform with the signal response $x_r(t)$. At those time sample points for which a peak in the convolution occurs, the sample point and the sign of the convolution are noted. A replica of the matched-filter waveform is scaled to the amplitude of the signal response, shifted in time to the sample point corresponding to peak correlation and subtracted from the signal response. This convolution and replica subtraction process is repeated until peaks corresponding to all possible interfaces have been found.

After detection, the relative values of the matched-filter correlation to the change in $\varepsilon_r$ are disproportionate due to the progressive signal attenuation through the ground as the distance from the GPR antenna increases. Ideally, a detection confidence value will be similar for detects that correspond to similar $\varepsilon_r$ changes regardless of distance from the GPR's antenna. To overcome this problem, a model of the media's attenuation characteristics needs to be developed. Deterministic equations have been developed that relate a media's permeability, $\varepsilon_r$, and attenuation[2]. While these equations may work well for known homogenous media, they are impossible to compute for dynamic data collections where the media's properties are unknown. Instead of calculating the expected attenuation using equations dependent on the media's characteristics, a simple attenuation model is generated directly from the data. This model is obtained by recording the maximum amplitude at each sample time across all traces in the data collection. It is unlikely that this attenuation model will have the monotonically decreasing curve shape required. Smoothing is done using irregular grid interpolation between the maximum monotonically decreasing peaks of the curve to obtain the desired shape. The reciprocal of the smoothed data is used to create a time-varying gain function. The matched filter correlation value of each detect is multiplied by the value of this gain function at the corresponding sample time index to obtain a confidence value. Finally, only the detects with the highest confidence values are kept, depending on the number of interfaces desired.

### 4.3 Prescreening

To characterize layer properties, GPR detections must be segmented according to the layer interfaces that caused them. However, to improve the computational efficiency and performance of the segmentation/tracking algorithms, a method for rejecting detects that do not belong to any substantial layer interface is needed. These rejected detects are considered to be clutter. To reject clutter, a nonsupervised classifier is used to determine which detects do not have properties of legitimate layers. Classifier performance is dependent on the separability of classes in some feature space. It is, therefore, desirable to obtain a set of features for each candidate detect that provides some separation between layers and clutter. For simplicity and robustness, two easily computable features are used. The first feature considers the spatial characteristics of the surrounding detect pattern and indicates the degree to which the shape fits that of a layer. The second feature is the detection confidence described earlier. The extraction of the layer indication features and the classifier procedures are explained in this section.

The layer indication feature is a combination of two complementary features. Both attempt to provide some general cue as to the probability that the detect of interest and surrounding detects have the spatial characteristics of a layer. The assumption made is that a legitimate layer will return a significant density of detects in the region of interest which have some general linear dependence with regard to position. The two features, which are summed to create the layer indication feature for classification, are a histogram indicator and a correlation indicator. Uncorrelated clutter returns have low values for both indicators

The histogram indicator feature is created using a histogram of the sample index of all the detects within a cross range window surrounding the detect of interest as illustrated in the top portion of Figure 3. The histogram represents the density of the points within a windowed range versus sample index. The density value at the sample index of the detect under test is used as a feature called the histogram indicator. The histogram indicator gives a high value for artifacts with well-defined horizontal characteristics, such as layer interfaces with minimal slope.

The correlation indicator provides better indication of sloped-layer interfaces. It considers the detects within a window around the detect under test. The feature value used is the absolute value of the correlation between the down-range sample index and the cross-range sample index of the group of windowed detects around the detect under test, as shown in the bottom of Figure 3. Detects from sloped layers will have a linear dependence between these indexes and, hence, a high correlation value. Returns from minimally-sloped layers tend to vary randomly around the mean detect index of the layer, creating a slightly lower correlation value for horizontal layers. Sloped layers typically are steep enough to provide a monotonic relationship between their indexes in spite of random variance in detect location and preserve high correlation values. The histogram indicator feature and the correlation indicator feature are added together to form the layer indicator.

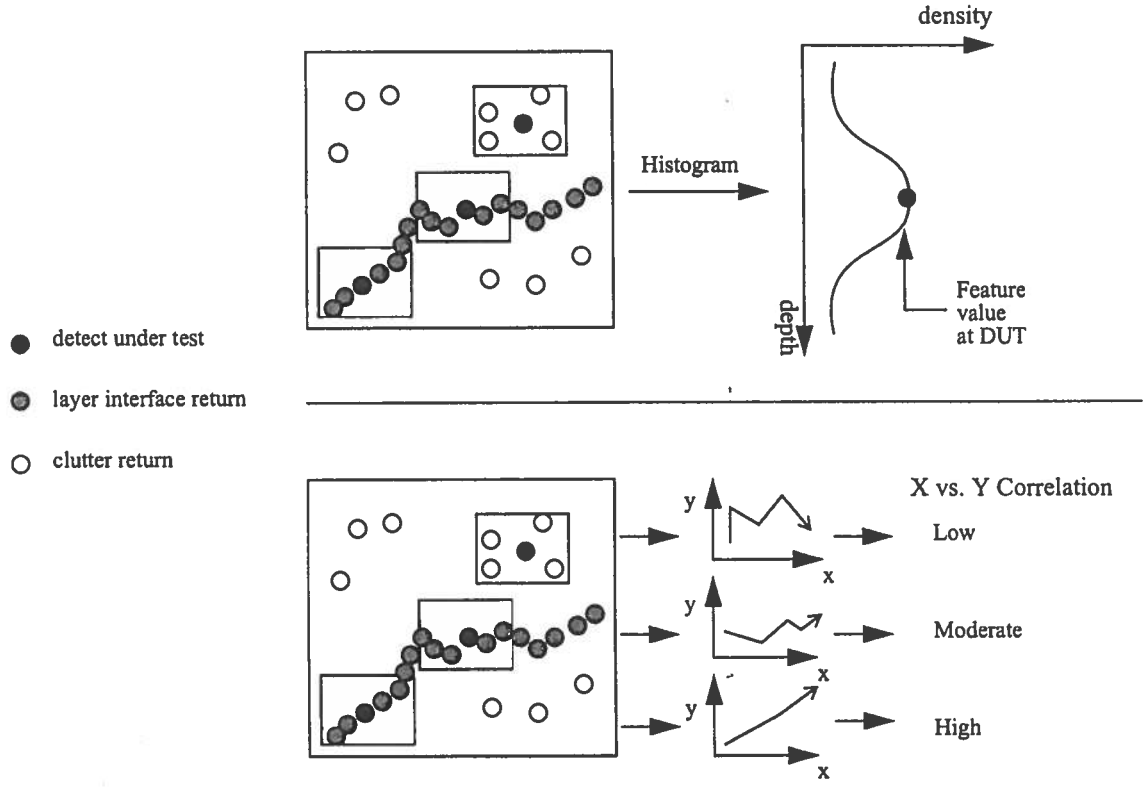


Figure 3. Histogram indicator (top), correlation indicator (bottom)

After the layer indicator feature and detection confidence are obtained, they are normalized and scaled to unity, creating the 2-D feature space for separating clutter from layer detects. The features are supplied to a K-means clustering algorithm which autonomously separates the clusters based on the minimization of a performance index[8]. In this case, the performance index is defined as the sum of the squared distances from all points in a cluster domain to the cluster center. K-means clustering segments the feature space to allow detects that have clutter characteristics (low values) to be discarded prior to track processing. Essentially, K-means provides an autonomous threshold selection based on the natural distribution of the detect features. The nonsupervised nature of this algorithm allows it to operate unmodified, regardless of the GPR system or collection configuration used.

### 4.4 Tracking

GPR operators can often associate groups of detects from a layer interface or anomaly by visual inspection. However, computers that process GPR data must have a way of associating layer interfaces and geophysical features together so that physical measurements and statistical analysis can be automated. The tracking algorithm assigns a unique label called a track number to groups of associated detects. The tracking algorithm is based on the weighted window searching and grouping procedure described by Cowdery[9], and operates on the detects that pass the prescreening stage.

After tracking is completed, there are often several separate tracks that can be identified as belonging to one consistent layer interface. Breaks in the tracks can occur due to misclassification of detects by the clutter rejection algorithm because tracking assigns track labels only to those detects that are not classified as clutter. Track joining works by considering the clutter detects as potential layer interfaces and assigning track labels where appropriate. By reassigning labels to these misclassified detects, track segments can be automatically joined together. The joining algorithm starts by performing an Euclidian distance search for nearby detects at the end of each track segment. The search is performed inside a windowed area determined by the tracking window sizes. If a non-tracked detect is found, it is assigned to the current track and the search begins again at the newly added detect location. When another track segment is found, it is relabeled with the track number belonging to the segment where the search was initiated. If no detects or tracks are found, the search moves to the next track segment.

Often, returns corresponding to legitimate layers are discarded by the detection algorithm. Track filling uses a windowed search from the start to end of each track segment and attempts to fill in any discontinuities along the length of the track segment using the locations of peak values from the received waveforms' matched-filter response. Track filling and joining increases track continuity in most cases.

## 5. LAYER PROPERTY ANALYSIS

Once layers have been segmented, properties of the layers may be computed. Of primary interest is the dielectric constant of the layer, which determines signal velocity in a medium and is combined with time-delay measurements to an interface for calculation of interface depth and layer thickness. Other calculations of interest may include statistical characteristics of layer thickness or depth, layer length, or perhaps even surface roughness and void content estimates. Arriving at the dielectric constant of layers is accomplished in different ways depending upon which GPR system configuration is utilized. Two methods/systems are used here: single-channel, air-launched, amplitude-based; and dual-channel, ground-coupled, time-based. Each system presents its own set of advantages, disadvantages, and processing requirements.

### 5.1 Air-launched system

The determination of layer thickness or anomaly location is a multi-step process that begins, directly or indirectly, with the computation of the reflection coefficient, $\rho$. At the boundary between two mediums (layers, voids, etc.) of differing $\varepsilon_r$, $\rho$ is the ratio of the reflected to incident electric fields. Neglecting multiple reflections at each boundary, we can relate $\rho$ at the boundary of layer $i$, $i+1$ to the received amplitudes using (2), where $\rho_0 = -A_o / A_m$ and $A_m$ is the peak amplitude of a flat metal plate response. The dielectric constant of layer $i+1$ can now be found using (3) where $\varepsilon_0$ = dielectric constant of air = 1. Finally, the layer thickness $d_i$ is found using (4) where $v_i$ is the velocity of propagation of the pulse in layer $i$ and $c$ is the speed of light.

$$\rho_{i,i+1} = \frac{A_i}{A_{i-1}} \cdot \frac{\rho_{i-1,i}}{1-\rho^2_{i-1,i}} \tag{2}$$

$$\varepsilon_{i+1} = \varepsilon_i \left[\frac{1-\rho_{i,i+1}}{1+\rho_{i,i+1}}\right]^2 \tag{3}$$

$$d_i = \frac{t_i - t_{i-1}}{2} \cdot v_i = \frac{t_i - t_{i-1}}{2} \cdot \frac{c}{\sqrt{\varepsilon_i}} \tag{4}$$

### 5.2 Ground-coupled system

Ground-coupled systems do not provide an accurate surface response from which amplitude measurements may be utilized in the dielectric calculations for successive layers. For this reason, an alternate method of determining the dielectric constant and signal velocity through each layer must be used. Time measurements through two signal-propagation paths may be used to compute the average velocity to a layer interface.

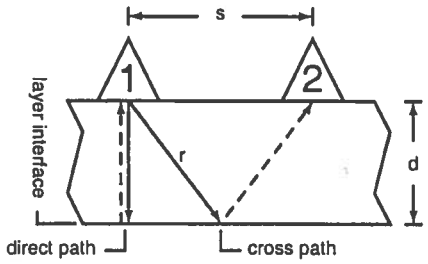


Figure 4. Dual antenna configuration

For a fixed geometry configuration, as shown in Figure 4, the separation distance between the antennas, $s$, and the travel time through each path are known, leaving only distance and velocity to each interface as unknowns. The direct path distance $r$ and cross path distance $d$ are given by (5) and (6), where $t_r$ and $t_d$ are the measured 2-way path propagation times. Both distance terms can be solved for in the two-equation system with the average velocity $v$ calculated using (7).

$$r = \left(d^2 + \left(\frac{s}{2}\right)^2\right)^{1/2} = \frac{vt_r}{2} \tag{5}$$

$$d = \frac{vt_d}{2} \tag{6}$$

$$v = \frac{s}{\sqrt{t_r^2 - t_d^2}} \quad \text{, where v is the average velovity.} \tag{7}$$

In applying this technique, subsurface profiles are collected through multiple propagation paths at each sample location.

Each channel of profile data is then independently processed by the detection and tracking algorithms. This results in detected interfaces in each profile. The time to an interface in each channel will be used to determine propagation velocity and depth; however, up to this point, no associations have been made between detects from an interface in one antenna channel (or path) and the detects from the same interface in the second antenna channel. It is, therefore, critical that some method pair together corresponding detects in profile data from each channel. Wave velocity, medium dielectric constant, and interface depth may then be calculated.

### 5.2.1 Matching tracks

Matching is a processing stage that is unique to the dual-antenna system. Layer dielectric constant is determined by utilizing time measurements through two wave propagation paths in the two-antenna system. This requires detected layers in the data from one antenna to be paired together with the corresponding detected layer in the data from the second antenna. An algorithm has been designed which autonomously performs this pairing based upon acceptable locations according to a range of possible dielectric values.

Calculations, given the system geometry, were performed to determine the range of acceptable delays between channels versus direct-channel sample time for an assumed range of dielectric values. From this range of acceptable delays between channels, a minimum cross-channel offset curve was determined. This curve provides the offset position of the matching window in the cross channel with respect to the sample position in the direct channel. The matching window size is also determined from the range of acceptable delays. The positions of tracked detects in the direct versus cross channels are compared to determine matched pairs. The algorithm biases matching towards the lowest $\varepsilon_r$ selection.

### 5.2.2 Depth calculation

To calculate the depth of each matched pair of detects, the detect location index in the two channels are used to reference a calibrated matrix of average $\varepsilon_r$ values, which are unique for a given pair of channel propagation times. The calibrated matrix was generated from testbed measurement calculations using materials with known $\varepsilon_r$ over a range of depth intervals. The average $\varepsilon_r$ obtained from the calibrated matrix is then used to determine the average velocity of the radar signal to the interface of interest. From this velocity and the time through either channel, the depth to the interface is computed.

### 5.2.3 Layer dielectric constant calculation

A parameter of interest is the dielectric constant, $\varepsilon_r$, of each detected layer. Only the average dielectric constant to each interface has been computed (to this point in the signal processing chain) because the time to each interface, as measured by the GPR, is a function of the average velocity of wave propagation to the interface of interest. The dielectric of the medium above an interface is, however, often more useful information than the average dielectric of all mediums above the interface. For this reason, an algorithm has been written that uses an iterative method, starting with the first layer and working down, to calculate an estimate of the dielectric of each individual layer. The algorithm assumes that the first matched pair in a given trace (a single GPR measurement of the subsurface at one location--sometimes called a profile; although, a profile may sometimes refer to a succession of traces stacked together to represent an area of the subsurface) is from the first-to-second layer interface; thus, the average dielectric constant is equal to the actual dielectric of the first layer. Once the first layer parameters have been established, the next layer (matched pair) is addressed. Given the depth and average dielectric to each interface and preceding layer, the dielectric constant of the layer may be calculated using (8) and (9) where *di*, *vi*, and $\varepsilon_i$ are the depth, velocity, and $\varepsilon_r$ respectively for each layer *i*. This process is successively followed for each interface in a trace.

$$v_i = \frac{[d_i - d_{i-1}]v_{i(avg)}v_{i-1(avg)}}{d_i v_{i-1(avg)} - d_{i-1}v_{i(avg)}} \tag{8}$$

$$\varepsilon_i = \left[\frac{c}{v_i}\right]^2 \tag{9}$$

## 6. DATA ANALYSIS EXAMPLES

A pair of GPR data collections using the ground-coupled configuration described earlier were recently completed in conjunction with two traditional airfield pavement evaluation surveys performed by AFSECA personnel. These collections provided a large set of ground-truthed GPR data needed for algorithm development, verification, and fine tuning. The large number of data files and other associated survey data obtained also prompted software interface adaptations to the GPR analysis software to provide more efficient processing, analysis and interaction with the large number of data sets. The figures below show data from one of these collections, along with the detected interface boundaries and plots of the calculated depths. The GPR analysis software was used to process and display the data, remove undesired detected interfaces, and generate the figures shown below in Figure 5.

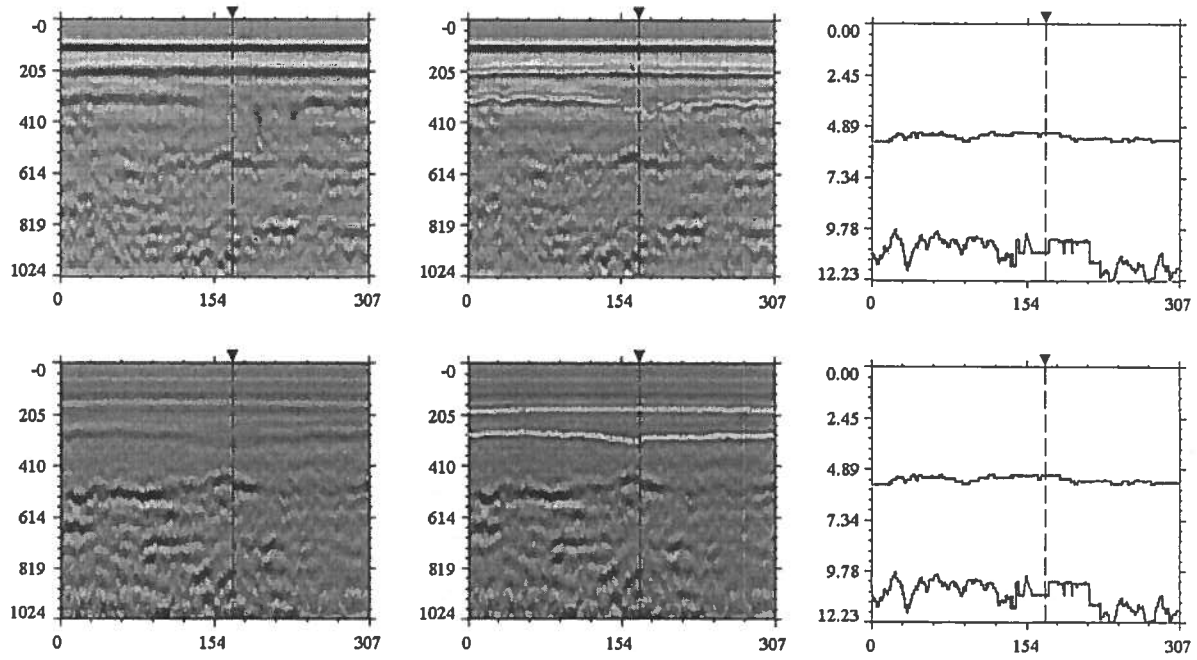


Figure 5. GPR data from airfield at McChord AFB. The two figures on the left show GPR data collected from a pair of ground-coupled antennas. The image on the top is from the direct channel and the image on the bottom is from the cross channel. The two figures in the middle show the same data sets with the first two detected layer interface boundaries over-plotted. The plots on the right show the calculated depth of the first two interface boundaries (note that due to the method used to calculate depth, the plots are identical). The black line and arrow in each of the figures represents the closest point in the data to a collected core sample. For this example, the thickness of the pavement core was 5.5 inches.

Examples of the GPR pavement thickness calculations versus nearby measured cores from the airfield evaluation at McChord AFB are shown in Table 1. The results were obtained after processing the GPR data using the algorithms described in this paper. The GPR analysis software was used to remove undesired detected interfaces and connecting non-continuous tracked segments, as necessary. For some data sets, layer interfaces can remain undetected due to either weak signal response (core 3) or interference from multiple thin layers (core 10). When the pavement interface can be detected, the calculated thickness values were close to core measurements.

Table 1. Measured core thickness vs. calculated GPR thickness from airfield at McChord AFB

| Core Number | Measured Thickness (In.) (nearest .25 In.) | GPR Calculated Thickness (In.) | Pavement Type | Notes |
|---|---|---|---|---|
| 1 | 12.0 | 11.87 | RPCC | Rebar noted 3.5 In. from top |
| 2 | 12.0 | 11.07 | RPCC | Rebar noted 3.5 In. from to |
| 3 | 11.50 | N/A | PCC | Pavement layer not detected in cross channel. |
| 4 | 11.75 | 11.74 | PCC | |
| 5 | 5.75 | 6.65 | AC | |
| 6 | 5.50 | 5.32 | AC | |
| 7 | 5.50 | 5.20 | AC | |
| 8 | 5.25 | 5.29 | AC | |
| 9 | 5.25 | 5.38 | AC | |
| 10 | 5.25 | N/A | AC | Pavement layer not detected in cross channel. |

RPCC - Reinforced Portland Cement Concrete, PCC - Portland Cement Concrete, AC - Asphaltic Concrete

## 7. SUMMARY

GPR has the potential the improve airfield evaluations by allowing more continuous and rapid assessment of pavement and subsurface properties. The signal processing methods described in this paper provide estimates of the properties of pavement and other subsurface layers. Large amounts of GPR data can be quickly processed and the results can be easily analyzed and summarized using the GPR analysis software. When favorable GPR conditions exist, the estimated pavement thickness is generally in close agreement with the measured values.

## ACKNOWLEDGEMENTS

This work was supported by the U.S. Air Force Research Laboratory Contract: F08637-00-C-7021.

## DISCLAIMER

The opinions, findings, and conclusions expressed in this publication are those of the authors and not necessarily those of the U.S. Air Force Research Laboratory.

## REFERENCES


1. U. S. Air Force, Airfield Pavement Evaluation Program, AFI 32-1041, April 1994.
2. D. J. Daniels, *Surface-Penetrating Radar*, The Institution of Electrical Engineers, London, 1996.
3. J. L. Kurtz, J. W. Fisher III, G. Skau, J. Armaghani, and J. G. Moxley, "Advances in ground penetrating radar for road subsurface measurements," SPIE Conference Proceedings on Radar Technology II, Orlando, FL, April 1997.
4. J. L. Kurtz, J. Cowdery, J. Meloy, and C. Overman, "Subsurface measurements utilizing the fusion of ground-coupled and air-launched GPR", SPIE Conference Proceedings on GPR II, August 2000.
5. T. Pagnoni, "An Automated Radar System for Non Destructive Testing of Bridges and Highway Pavements," Sixth International Conference on Ground Penetrating Radar, Tohoku University, Sendai, Japan, October 1996.
6. P. Beckman and A. Spizzichino,*The Scattering of Electromagnetic Waves from Rough Surfaces*, The Macmillian Co., New York, pp. 316-333, 1963.
7. J. W. DiFranco and W. L. Rubin, *Radar Detection,* Artech House, Inc., Dedham, Massachusetts, pp. 214-219, 1980.
8. C. M. Bishop, *Neural Networks for Pattern Recognition*, Oxford University Press Inc., New York, pp 187-189, 1995.
9. J. M. Cowdery and J. L. Kurtz, "Ground penetrating radar signal processing techniques for road subsurface measurements", SPIE Conference Proceedings on Radar Technology IV, Orlando, FL, April 1999.